



New insights on fracture roughness and wall mismatch in carbonate reservoir rocks

M. M. Al-Fahmi^{1,2}, Sait I. Ozkaya³, and Joe A. Cartwright¹

¹Department of Earth Sciences, University of Oxford, S Parks Road, Oxford, OX1 3AN, UK

²Aramco Overseas Co., 10 Portman Square, London, W1H 6AZ, UK

³GeoScience Consultant, OGS WLL, Manama Center, P.O. Box 18665, Manama, Bahrain

ABSTRACT

Roughness and mismatch of fracture surfaces (walls) are key hydromechanical rock properties that influence (or control) how the rock masses slide and the ways in which fluids permeate the structure. Fracture roughness has been studied for decades from outcrop fractures and experimental analogues because it is difficult to detect and describe roughness of reservoir rock fractures in the deep subsurface. Here, we present new insights about roughness and wall mismatch of opening-mode fractures (hereinafter fractures) in deep carbonate reservoir rocks using a combination of new measuring techniques. The fractures are described from core and modern electrical borehole imaging data that were obtained from extended-reach drilling into the Arab oil reservoir rocks in Eastern Arabia. The fractures, both unfilled and calcite-filled fractures, exhibit moderate and high roughness, ranging between 5 and 15 on the joint roughness coefficient scale. Most fractures exhibit matching walls, permitting use of the cubic law for fluid-flow modeling. Some unfilled fractures exhibit mismatching walls that preserve their apertures under compression of the current stress field in Eastern Arabia. Roughness and mismatch of fracture walls were found to reflect the fabrics of host carbonates and hence are potentially predictable from analyses of carbonate lithological facies (lithofacies).

INTRODUCTION

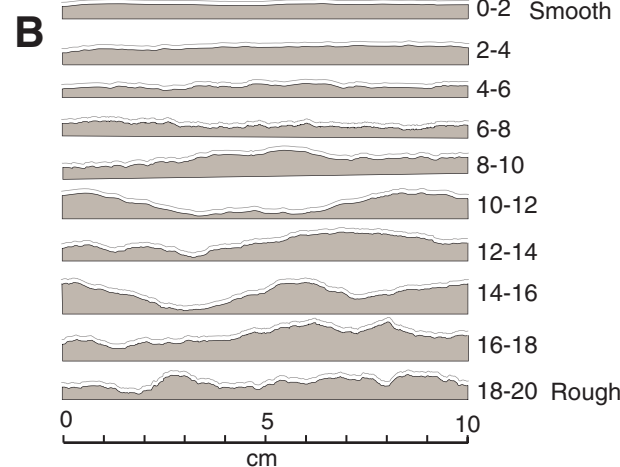
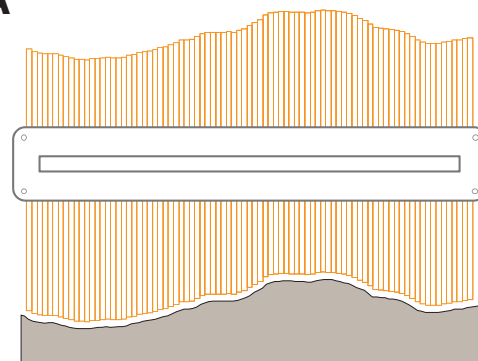
Fracture roughness refers to the degree to which undulations occur along fracture surfaces (e.g., Barton and Choubey, 1977; see also Figs. 1A, 1B). Mismatch of fracture walls refers to the degree of deviation from perfectly interlocking (matching) walls (e.g., Zhao, 1997; see Figs. 1C, 1D). Roughness and mismatch of fracture walls are key hydromechanical properties in the rock shear strength and hydraulic conductivity (permeability) of rock masses (e.g., Barton et al., 1985; Olsson and Barton, 2001). Measurement of rock strength and permeability is an important topic in a wide range of scientific research and industrial applications. Relevant fields include geotechnical, hydrological, and petroleum reservoir sciences as well as geophysical imaging of subsurface fractures.

Roughness measurements have been extensively and almost exclusively reported from numerical simulations, laboratory experiments on artificial fractures, and fractures and faults in near-surface rocks (e.g., Barton and Choubey, 1977; Maerz et al., 1990; Brown, 1987; Tatone and Grasselli, 2010; Candela et al., 2009; Sagy et al., 2007; Schmittbuhl et al., 1993). Roughness measurements on deep reservoir fractures are rare, possibly due to inadequacy of direct data on roughness and/or lack of efficient measuring techniques. Rationally, direct roughness measurements are unattainable using the various subsurface data sources other than core—assuming it is in good quality and from boreholes that were geometrically ideal to intersect with reservoir rock fractures.

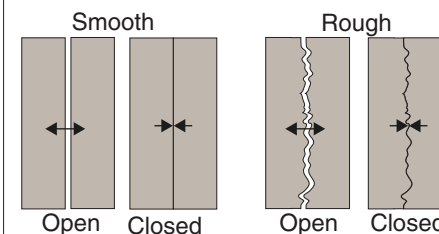
Here, we present new measurements and insights on the nature of roughness and wall mismatch of carbonate reservoir fractures. The fractures are described from outstanding data sets of directional core combined with high-resolution electrical borehole imaging. The data sets were obtained from extended-reach drilling into the Arab carbonate reservoirs, the world's most prolific and producing hydrocarbon-bearing rocks. The drilling site is a well-studied hydrocarbon field of a dome structure that is located within the tectonically active region of Eastern Arabia (e.g., Al-Fahmi et al., 2016; Ameen, 2014; see also Fig. 2). Roughness measurements were obtained by applying new quantitative nondestructive techniques on fracture profiles digitized from high-definition optical scans of the core. The results from core data were correlated with the detection levels of fractures and aperture measurements from corresponding borehole images. The results bear implications on the modeling of fracture permeability and sliding potential in subsurface carbonate reservoirs.

GEOLOGIC BACKGROUND

The data sets were obtained from two directional boreholes (X-01 and X-03) that were drilled into the Upper Jurassic Arab carbonate reservoirs (A, B, C, and D). The drilling targeted the reservoirs located at ~1.4 km below surface in a hydrocarbon field of a low-relief dome in Eastern Arabia (Al-Fahmi et al., 2016, 2014). Each reservoir consists of a shallowing-upward marine sequence of a variety of lithofacies, including mudstones, wackestones, packstones, skeletal grainstones, ooid grainstones, and dolomites (e.g., Mitchell

A Fracture wall roughness**C** Fracture wall matching and aperture

Wall matching



Wall mismatching

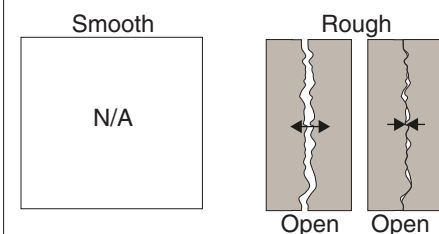
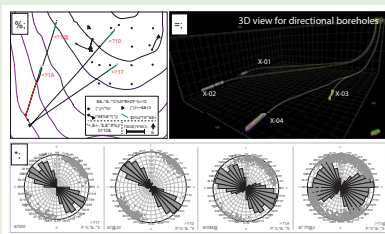


Figure 1. (A) Barton's profile comb, which is used widely in roughness measurements of artificial fractures and near-surface rock surfaces. (B) Typical profiles of joint roughness coefficients (JRCs) that are commonly used in rock mechanics to relate roughness to shear strength. The values of fracture roughness that were obtained for the Z_z roughness parameter were converted to the JRCs because they provide a visual reference for the empirical and standard relationships to the fracture hydromechanical properties (e.g., Barton, 2013). (C) illustrations of wall mismatch and the dependency of fracture aperture on the degree of wall mismatch in smooth and rough fractures under stress conditions that open and close fracture walls. Wall mismatch is not expected in smooth fractures because it is only obvious in mismatched rough walls.



'Supplemental File. Further analysis of data sets. Please visit <https://doi.org/10.1130/GES01612.S1> or the full-text article on www.gsapubs.org to view the Supplemental File.

et al., 1988). The porosity averages ~15%, ranging in type from interparticle to moldic to vugular (e.g., Mitchell et al., 1988).

Carbonate reservoir fractures in Eastern Arabia were interpreted from borehole images of the directional boreholes that were drilled for oil and gas extractions from the Arab, Hanifa, Khuff, and other reservoirs (Ameen, 2014; Ameen et al., 2010; MacPherson and Ameen, 2014; Luthy and Grover, 1995; Thagafy et al., 2017). The fractures are generally grouped based on their strikes into east-west (E-W), northeast-southwest (NE-SW), and northwest-southeast (NW-SE) regional systems (e.g., Ameen et al., 2010; Ameen, 2014). The NE-SW and E-W systems are optimally oriented to the present-day maximum horizontal principal stress (S_{Hmax}) in Eastern Arabia

(Ameen et al., 2010; Ameen, 2014). The S_{Hmax} has an estimated ~60° and 100° azimuth from analyses of breakouts and wall-tensile fractures in boreholes in the Arab, Hanifa, and Khuff reservoirs (e.g., Ameen et al., 2010; Alghamdi et al., 2016; Thagafy et al., 2017). The S_{Hmax} is recognized to be higher than the vertical stress (S_v) of the sediment load, generating a strike-slip stress regime in the region, due to the active tectonic compression of the Arabian-Eurasian plate collision (e.g., Ameen, 2014).

The data sets in this study show that the Arab reservoir fractures exist in two systems: 80% unfilled fractures, and 20% calcite-filled fractures (Figs. S1 and S2 in the Supplemental File¹). The two systems are opening-mode fractures with normal dips to the nearly flat strata. After comparing observations

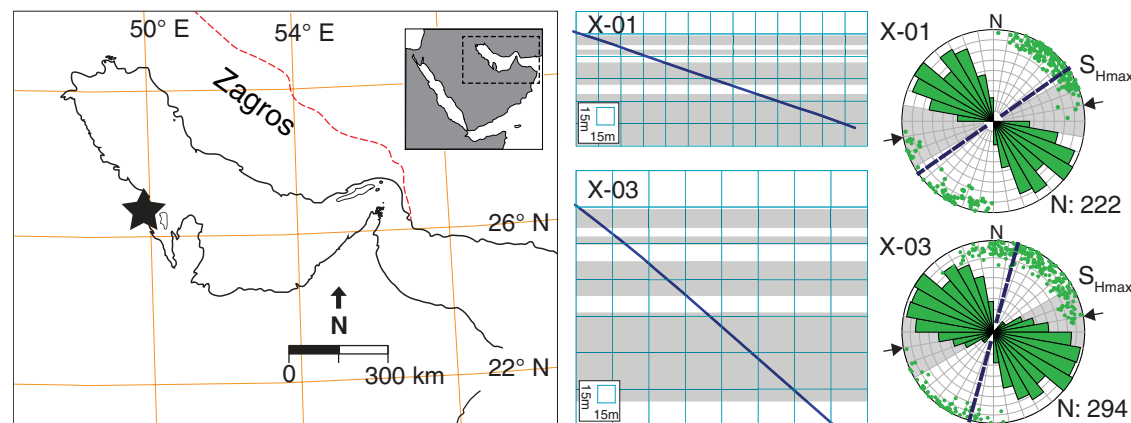


Figure 2. (Left) Map of the study area in Eastern Arabia. (Center) Two cross sections for the directional boreholes (X-01 and X-03) that were used to obtain core and borehole images from the Arab carbonate reservoirs (gray strata). (Right) Stereonets combined with rose histograms of the fracture strikes and dips. The fractures are mostly part of the NW-SE system due to the biases of borehole orientation presented with the directions of borehole orientations (dashed lines) and the S_{Hmax} (arrows and gray shading).

from the core and borehole images, 80% of unfilled fractures are missing from the borehole images in X-01 and 45% are missing in X-03 (Al-Fahmi and Cartwright, 2015). The boreholes (X-01 and X-03) intersected a NW-SE system, and X-03 additionally intersected E-W and NW-SE systems (Fig. 2). Fracture strikes indicate that the boreholes missed the fractures that are nearly parallel to the boreholes, but the fracture strikes from all drilled boreholes in this region resemble the NW-SE, E-W, and NE-SW fracture systems that were previously recognized in the carbonate reservoirs in Eastern Arabia (Fig. S1 in the Supplemental File [footnote 1]).

METHODS

Fracture roughness has long been described using various empirical, statistical, and fractal methods (e.g., Tatone and Grasselli, 2010; Weissbach, 1978; Lee et al., 1990; Barton and Choubey, 1977; Schmittbuhl et al., 1993; Haneberg, 2007). Among these methods, roughness is widely described by visually comparing two-dimensional (2-D) profiles of fracture surfaces to 10 typical profiles using joint roughness coefficients (JRCs; Fig. 1A; Barton and Choubey, 1977). The values of the JRCs range on a scale from 0 (very smooth) to 20 (very rough; Barton, 2013). Roughness has been also described numerically using statistical parameters that were proposed to overcome the simple and subjective nature of the visual techniques (e.g., Tatone and Grasselli, 2010; Li and Zhang, 2015). Nevertheless, the visual and statistical techniques cannot be used to measure roughness and wall mismatch of filled and unfilled fractures in a cylindrical directional core. The visual techniques are limited in use to the unfilled fractures. Walls of filled fractures are not accessible, and breaking core or dissolving mineral

fills to precisely expose the host rock walls is unfeasible. Furthermore, the available statistical techniques require presenting core fractures in a digital format of flattened profiles from their actual different elliptical traces around the core circumference.

To overcome these challenges, we used a novel combination of efficient and nondestructive techniques to describe roughness and wall mismatch of fractures. The techniques provide a solution that allows both types of filled and unfilled fractures from geometrical core to be described. The core was scanned using an industrial scanner, which produced 360° optical images of core circumference in true color with a resolution of up to 10 pixel/mm, and details up to 40 pixel/mm. Calcite-filled and unfilled fractures were then digitized from the optical scans up to 0.1 mm (measuring resolution) of core dimensions using a computer-aided design (CAD)-based commercial software (Fig. 3). It was not possible to extract precise profiles for the core fractures using image-processing techniques such as pattern recognition and edge detection, so the fracture digitization was done manually.

The shape of a digitized fracture profile resembles a sine wave produced by the intersection plane of the fracture with the drill-core cylinder (Fig. 3B). The shapes of digitized profiles encompass information about fracture geometry (strikes, dips, amplitude, and roughness) and intersection with the core geometry (strike, dip, height, and diameter; Fig. 3). The lengths of fracture profiles vary according to their elliptical intersection perimeters and mostly range between 25 cm and 35 cm.

Numerical techniques were then developed in a spreadsheet-based application to measure the profile deviations in x-y space from a fitting smooth curve (Fig. 3B). The techniques can compute statistical parameters of fracture roughness such as Z_2 , where Z_2 is among several numerical parameters that have been used to describe profile undulations (e.g., Myers, 1962; Tatone and

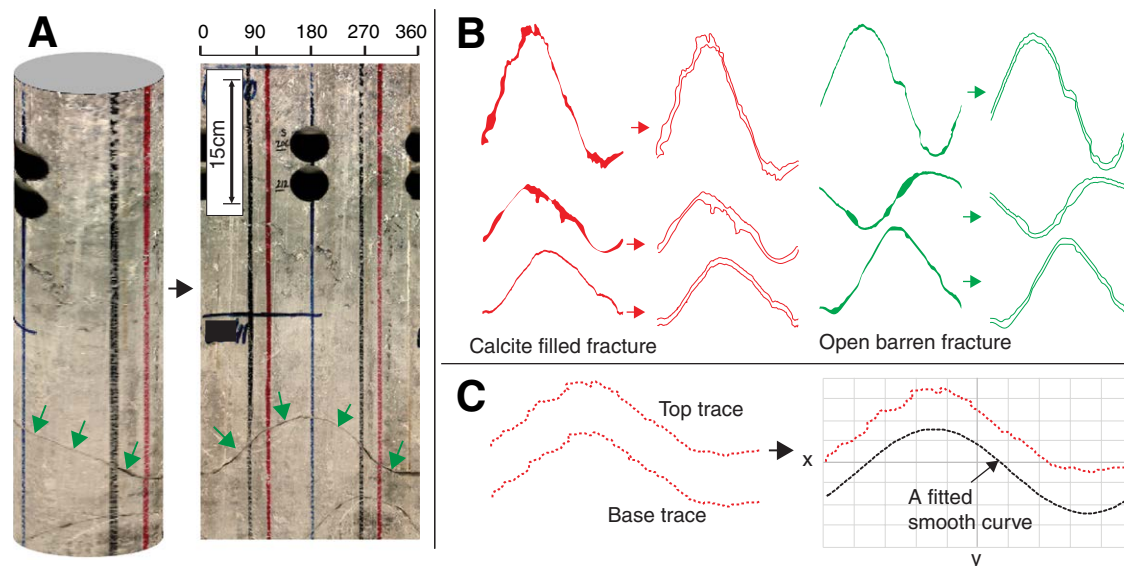


Figure 3. (A) Core sample with an unfilled fracture (green arrows) cutting the core; the core sample was unrolled as a 360° photographic scan, and the core scans were used to trace and digitize fractures up to 0.1 mm of core dimension. (B) Six examples of digitized profiles of calcite-filled fractures (red) and unfilled fractures (green) and their separated top and base profiles. (C) Top and base profiles of a digitized fracture and demonstration of how it was used to measure roughness by computing the Z_2 parameter of the profile deviations in x-y dimensions from a fitted smooth curve. Note: The lines in the core in A are markers for core handling at the laboratory, and the two black holes are sampled plugs.

Grasselli, 2010). The Z_2 parameter measures the root mean square of the first derivative of the surface profile from a centerline average:

$$Z_2 = \left[\frac{1}{L} \int_{x=0}^{x=L} \left(\frac{dy}{dx} \right)^2 dx \right]^{1/2}. \quad (1)$$

The measured Z_2 values can be converted to the JRCs and other numerical parameters using established relationships (e.g., Li and Zhang, 2015). Other statistical parameters of roughness and their relations to the JRC scale are also possible to use in the same fashion. The Z_2 values were converted to the JRC scale using the following relationship (e.g., Li and Zhang, 2015):

$$JRC = 55.7376Z_2 - 4.1166. \quad (2)$$

JRC values are preferred here because values of typical JRC profiles provide visual references that can be correlated to the rock hydromechanics using empirical relationships (e.g., Barton, 2013).

The wall mismatch was analyzed using three different methods and analyzing top and bottom profiles (profile pair) of each fracture (Fig. 3B). The first method estimates the difference in JRCs between profile pairs. The second method calculates the standard deviations of apertures (STDEV-A) between profile pairs after flattening and resampling the profile pairs (Fig. 3C) to be at the same x-y coordinates. The third method uses the flattened and resampled profiles for a quantitative correlation, from which we can relate mismatch co-

efficients (MCs) ranging between 0 and 1, where 0 indicates perfectly matching fracture walls.

The obtained measurements on roughness were correlated with the host-rock lithology, which was described in detail (~5 cm interval) from core and sections following a modified version of Dunham's classification (Dunham, 1962). In addition, the measurements were correlated to the results obtained from borehole imaging of unfilled fractures using two different methods: (1) calculations of mechanical and hydraulic apertures, and (2) correlations between apertures and fracture strikes. These measurements were performed to evaluate if fracture apertures were sensitive to the stress field and stress-dependent permeability in the subsurface.

Mechanical and hydraulic apertures of the fractures were measured from the borehole images using the methods described in Luthi and Souhailé (1990). The mechanical aperture of a fracture is the size of the fracture opening between the fracture walls. The hydraulic aperture of a fracture is related theoretically to the fracture mechanical aperture, roughness, and pressure gradients of fluid flow (Barton et al., 1985). The measuring methods of apertures are available in the software applications (e.g., Techlog) that are used in processing and interpretation of borehole images. The fracture mechanical aperture (W) from borehole images was calculated (in mm) by this relationship:

$$W = cAR_m^b R_{xo}^{1-b}, \quad (3)$$

as a function of the integrated additional mud current A , the resistivity of the formation R_{xo} , and the resistivity of the mud R_m , with the measuring tool-dependent coefficients b and c (Luthi and Souhaité, 1990). Mean mechanical aperture (W_m) of a fracture was calculated as:

$$W = \frac{\sum W^3 n}{n}, \quad (4)$$

with the sum of apertures (W ; from sampled points) along the fracture trace averaged over the fracture length (n) in borehole (e.g., Luthi and Souhaité, 1990). The mean hydraulic aperture (W_h) from borehole images was calculated as:

$$W_h = \sqrt[3]{\frac{\sum W^3 n}{n}}, \quad (5)$$

i.e., the cubic mean of the mean of the cubes of mechanical aperture. This calculation method is provided by the imaging tool manufacturer based on production data, and as such, the hydraulic aperture is equal to, or greater than, mechanical apertures if fracture walls are not perfectly matching. This calculation differs from the rock mechanical methods, in which hydraulic aperture is expected to be either equal to or smaller than the mechanical aperture if fracture walls are mismatching (e.g., Barton et al., 1985).

RESULTS

Fracture roughness measurements are summarized in Figure 4A. About 95% of the Z_2 measured values range between 0.08 and 0.24. The Z_2 values are normally distributed, with equal JRCs ranging between 5 and 15 for both filled and unfilled fractures (Fig. 4A). Measurements of wall mismatch are presented in Figure 4B. Most fractures exhibit mismatch coefficients less than 0.1. A few fractures have noticeable degrees of mismatch. Results from calculating the standard deviation (SD) of apertures show that about two thirds of fractures have less than 0.15 SD. The remaining third ranges between 0.15 and 0.4 SD. The limited occurrences of wall mismatch resulted in weak relationships between the JRCs and correlation coefficients as well as the standard deviations of apertures.

The unfilled fractures in coarse-grained lithofacies exhibited profiles rougher than the fractures in fine-grained lithofacies (Fig. 4C). These observations were similar for the calcite-filled fractures (Fig. 4C). This relationship between roughness and lithology was more obvious in the limestone fractures than in the dolomite fractures (Fig. S3 in the Supplemental File [footnote 1]). The roughness generally increased with the increasing grain size of host limestone. The probability of finding wall mismatch, although limited, seemed to increase with increasing grain and pore size of host limestone rocks.

The aperture measurements from borehole images displayed separation between mechanical and hydraulic apertures (Fig. 4D). In addition, the size of apertures varied along the profiles of unfilled fractures in borehole images (Fig. S4 in the Supplemental File [footnote 1]). In addition, the mean apertures displayed comparable trends from both boreholes, with increasing apertures

toward the fractures striking E-W and NE-SW ($\sim 60^\circ$ – 100°), and decreasing toward the fractures striking NW-SE ($\sim 120^\circ$ – 180°).

DISCUSSIONS AND IMPLICATIONS

Nature of Roughness and Predictions

The fractures exhibited a moderate to high range of roughness magnitudes on the JRC scale between 5 and 15. The range of roughness measurements was comparable for unfilled and calcite-filled fractures, despite the fact that the two fracture systems differ in their diagenesis history. The roughness is apparently independent of the fracture mineralization process. Mineral fills are well-preserved casts for paleofracture roughness of fracture walls. The fractures (smooth and rough) have generally matching walls, and only a minority of the rough fractures exhibited an obvious wall mismatch. Therefore, the parallel-plate approach (the cubic law) is practical for estimating fluid flow in these reservoir fractures.

The roughness and mismatch of fracture walls are clearly products of the variations in sizes and shapes of the matrix, grains, crystals, and pores of host carbonates (Fig. 5A). The limestones and dolomites of the Arab carbonate reservoirs exhibit both primary and diagenetic fabrics (e.g., Mitchell et al., 1988). The statistical distributions (Figs. 4A and 4B) reveal the probability of sampling different lithological beds from fine-grained to coarse-grained beds. High values of roughness and wall mismatch are more common from coarse-grained rock than from fine-grained rock of small sizes of pores (Fig. 4C). The observed wall mismatch can be noted here as fabric-dependent, to make a distinction from the wall mismatch occurring due to wall slips in sheared fractures (faults; Barton et al., 1995). Fabric-dependent roughness and wall mismatch are potentially predictable from limestone lithological descriptions. The Arab reservoir rocks exhibit a wide range of limestone lithofacies, such as mudstone, wackestone, packstones, grainstones, floatstone, and rudstone (e.g., Mitchell et al., 1988). Some, if not all, of these lithofacies exist in other carbonate reservoirs. Nonetheless, the prediction of roughness magnitudes from lithological fabrics involves some assumptions about fracture heights. The prediction is possible for multi-lithofacies carbonates, where the mechanical stratigraphy typically bounds fracture heights (Fig. 5C). The through-going fractures (that cut through various lithological layers) are expected to display a roughness stratification (i.e., roughness anisotropy with the vertical direction normal to the strata horizontal planes). The measured magnitudes of fracture roughness are considered static, which means that the core-based measurements are representative of the magnitudes of reservoir fracture roughness. Two reasons can be listed here to support this consideration. First, the texture, porosity, mineralogy, and mechanical properties of the Arab reservoir rocks are not stress-sensitive, (i.e., these properties do not change under the reservoir stress conditions; Ameen et al., 2009). Second, the core did not exhibit distortions in the pore-scale architecture, such as the breakages of grain bonds, or cracks that can be considered signs for the confining stress removal (unloading).

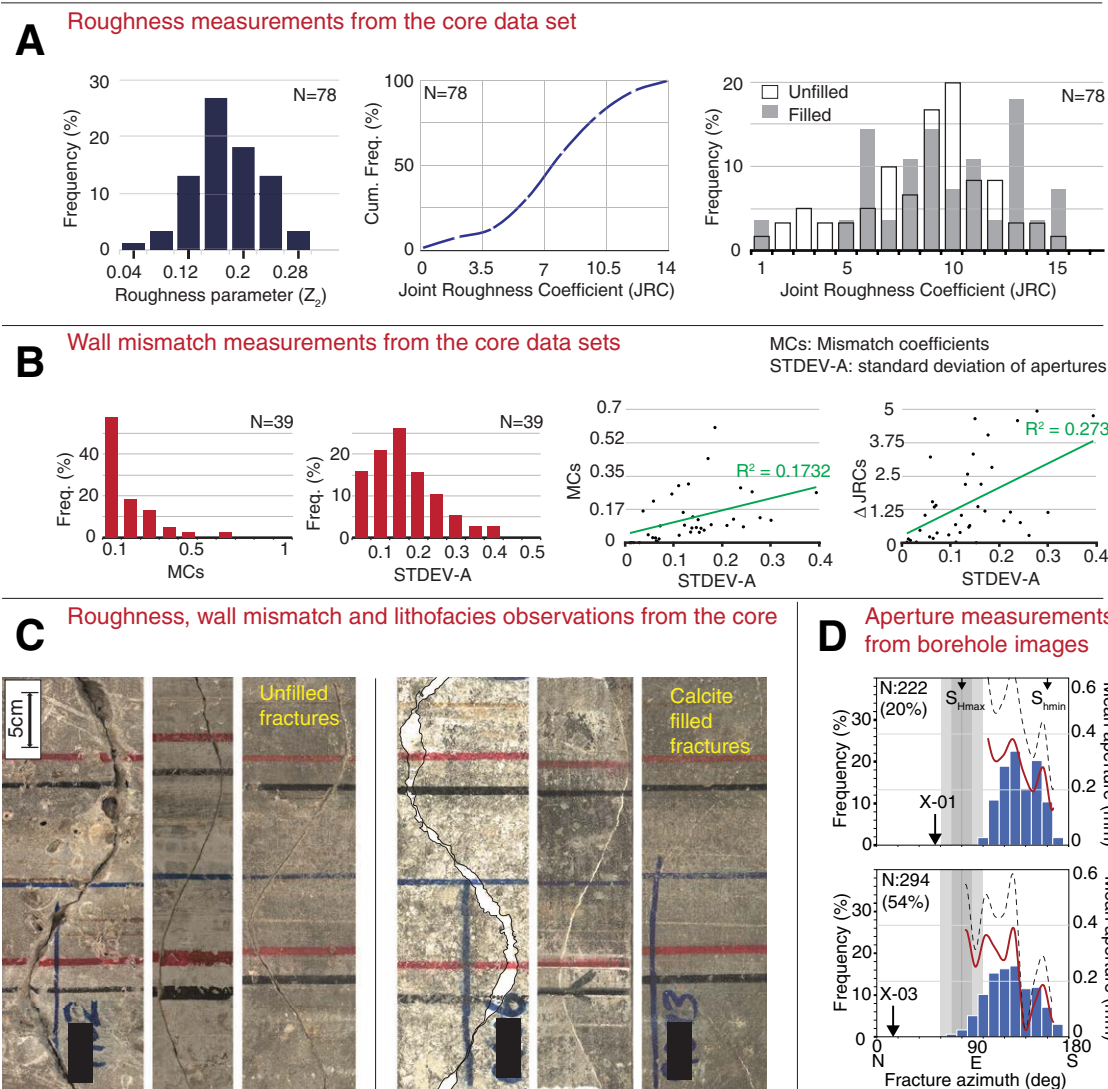


Figure 4. (A) Three figures for roughness statistical distributions; the first shows measurements of the Z_2 roughness parameter of the fractures (calcite-filled and unfilled fractures), the second shows the Z_2 values after conversion to joint roughness coefficients (JRCs), and the third shows the JRCs for calcite-filled and unfilled fractures (both fracture systems exhibit similar JRCs between 5 and 15). (B) Four figures for statistical analyses of the fracture wall mismatch; the first is a statistical distribution of mismatch coefficients (MCs) that demonstrates that fracture walls are mostly matching ($MC \approx 0$) and that a minority of the fractures have mismatching walls ($MCs > 0.2$), the second is a statistical distribution of the standard deviations of apertures (STDEV-A) that demonstrates a very limited deviation from a matching wall (two thirds of fractures have less than 0.15 SD), and the third and fourth figures are correlations (cross plots) among the MCs, JRCs, and STDEV-A that demonstrate weak relationships due to limited occurrences of wall mismatch. (C) Core photographic scans of filled and unfilled fractures of walls ranging from mismatching rough to matching smooth. (D) Measurements from the borehole images demonstrating the mean mechanical apertures (red curve) and mean hydraulic apertures (dashed curve) of the unfilled fractures that are presented in the rose diagrams in Figure 1. See the text for further details.

Roughness Effects on Fracture Aperture

The effects of fracture roughness and wall mismatch on aperture of unfilled fractures are apparent from analyses of borehole images. There are two important results supporting these interrelated effects on apertures. First, wall mismatches of fractures are obvious from the variation in aperture size along the profiles of

detected fractures in borehole images. The sum of these aperture variations is visible from the separations between the mean mechanical and mean hydraulic apertures (Fig. 4D). Second, the mean apertures (hydraulic and mechanical) generally increase toward the fractures optimally oriented to the S_{Hmax} ($\sim 60^\circ$ – 100°), and they decrease toward the fractures striking NW-SE ($\sim 120^\circ$ – 180°), as their walls (oblique and perpendicular to the S_{Hmax}) are closed under the compressive

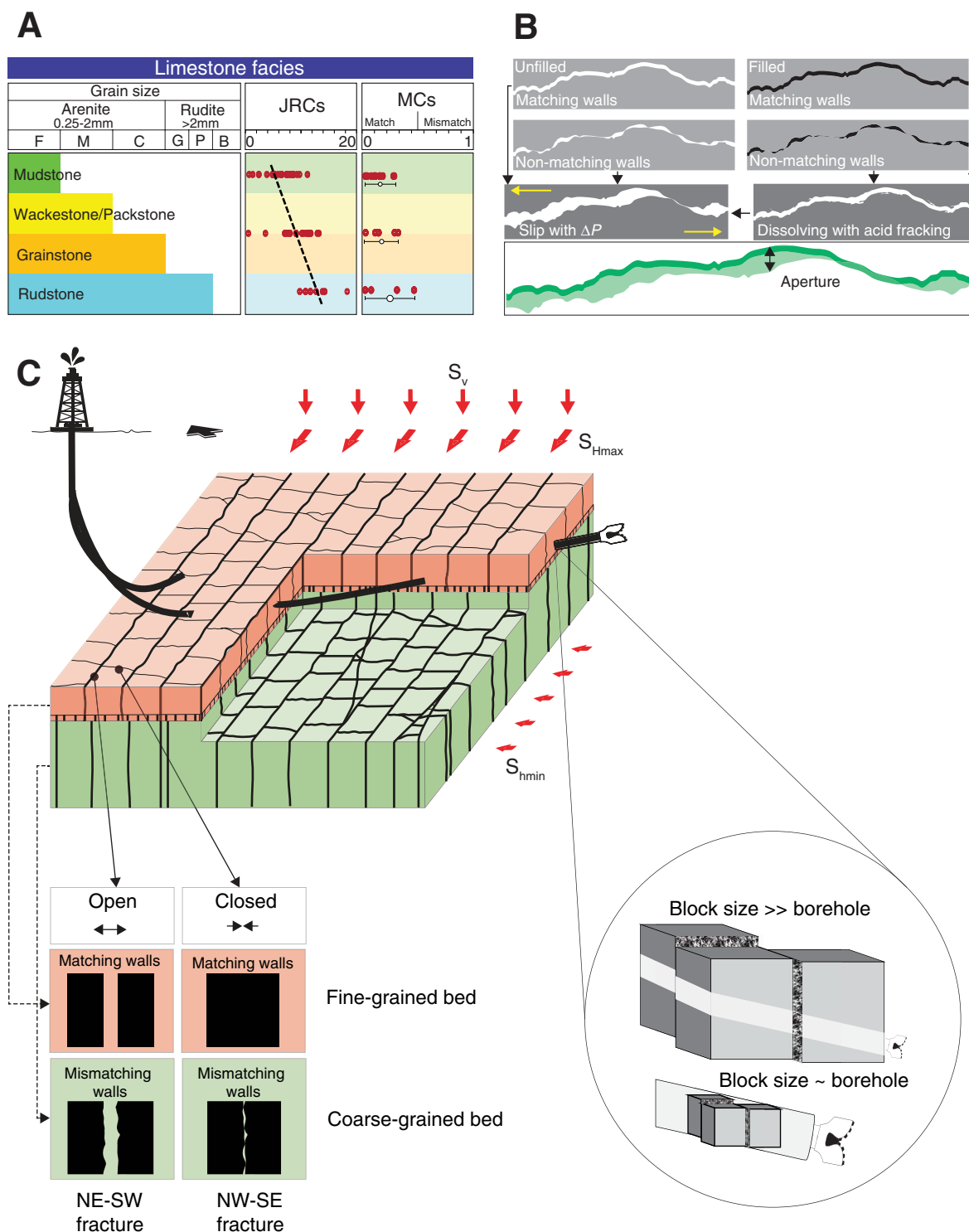


Figure 5. (A) Plots comparing the joint roughness coefficients (JRCs) and mismatch coefficients (MCs; red circle) of fracture roughness and wall mismatch with the limestone lithofacies of the Arab reservoirs described based on Dunham classification. The plots display a general increase (averaging line) in the roughness magnitude with increasing grain size and pore size, as can be characterized from the lithofacies hierarchy, from fine-grained (muddy rock) to coarse-grained (grainy, skeletal, and vuggy) rock. F—fine; M—medium; C—coarse. (B) Different possible paths of rough apertures that may evolve from filled and unfilled fractures under the geological conditions and reservoir production dynamics. (C) Framework model for two carbonate beds of different lithofacies that are cut by the NE-SW and NW-SE regional systems of unfilled fractures in subsurface carbonate reservoirs in Eastern Arabia. The model demonstrates that the NW-SE fractures in coarse-grained beds have apertures despite the fact that their walls are closed under the present-day S_{Hmax} caused by tectonic compression. Other related subsurface parameters that bear implications for the directional borehole stability are considered in the framework, such as size of fractured blocks. Small blocks can be displaced to fall in the boreholes according to the equilibrium between load of gravity (S_v) or tectonics (S_{Hmax}), roughness, and friction. G—granule; P—pebble; B—boulder.

stress in Eastern Arabia. The fracture apertures are dynamic under the stress field due to the fact that tensile strengths of barren fractures are typically zero (i.e., the fracture walls are not bonded by minerals). Because the S_{Hmax} and the dominance of fractures with matching walls, ~80% of the core unfilled fractures could not be detected in the corresponding borehole images of X-01. The majority of these NW-SE fractures are closed under the compressive stress. The minority of fractures (~20%) that were detected from X-01 had wall mismatches preserving apertures between fracture walls under this compressive tectonic regime. The unfilled fractures were detected because their apertures (and hence permeability) were susceptible to the infiltrated drilling mud. Calcite-filled fractures exhibited high resistivity in borehole images, indicating they are impermeable to the infiltrating drilling fluid. These observations indicate that in situ permeability of fractures is ineffective if fractures are mechanically closed along complete (matching) wall contacts, or sealed completely with impermeable minerals like calcite cements (Figs. 5B and 5C). Dissolving calcite, however, by acid fracking can potentially make the calcite-filled fractures with wall mismatch as permeable as unfilled fractures (Fig. 5B).

Roughness Effects on Rock Strength

It is not possible to describe the effects of fracture roughness on reservoir rock strength (i.e., the strength of the intact rock blocks and freedom of block movement) for deeply buried rocks. In the absence of observations, we can only relate the possible effects of roughness from previous empirical studies. Rock strength is an important factor in planning, drilling, and completing boreholes, especially the directional drilling boreholes that cost millions of dollars. In general, lower JRCs bear the highest potential of sliding (e.g., Barton, 2013) and hence may risk the stability of directional boreholes (Fig. 5C). The sliding potential can be correlated to slope instabilities; the rougher the fracture surface, the lower is the sliding potential (e.g., Younessi and Rasouli, 2010). The drilled boreholes (X-01 and X-03) did not have any signs of instability issues such as collapse or tight holes. However, some fractures may slip in critically stressed environments and under the dynamics of reservoir production and injection (Zoback, 2007; Fig. 5B). Some considerations must be given, besides roughness, to the shapes and sizes of fractured rocks (blocks). Fractured blocks that are smaller than borehole sizes can slide and fall into the borehole (Fig. 5C). The blocks that are larger than the borehole size cannot be displaced into the boreholes, and their movement can only happen tectonically on moving faults. Some considerations must also be given to internal friction angles, bonding strengths of calcite filling, and the setting with regard to the effective stress field and borehole geometry (Fig. 5C).

Roughness Effects on Fracture Detection

The effect of fracture roughness and wall mismatch on geophysical detection methods of subsurface fractures can be related from borehole images.

Borehole imaging is the mostly utilized geophysical method for measuring fracture orientation, abundance, and apertures in subsurface reservoir rocks. Fracture roughness and wall mismatch are among the major factors influencing the borehole imaging capability used to detect or miss carbonate reservoir fractures (Al-Fahmi and Cartwright, 2015). The sizes of unfilled fracture apertures are dynamic, depending on the roughness and wall mismatch of fracture walls as well as the compressive stress field. The wall mismatch, especially of rough fractures, contributed to the relatively large fracture sizes and preserved apertures in the fractures in Eastern Arabia, which are under stress in the current tectonic compression. Accordingly, these fractures are easily detected and measured in borehole images. Wall-matching fractures that are closed under the compressive stress field (i.e., lack apertures for infiltrating drilling mud) are undetected in borehole images. This situation contributed to the inconsistency and reduction in estimating fracture abundance by borehole images. The variations in fracture aperture sizes due to wall mismatch and stress field contribute to the reservoir rock anisotropy, which affect geophysical measurements for reservoir electrical, acoustic (seismic), and fluid-flow properties.

CONCLUSIONS

We presented new insights about roughness and wall mismatch of opening-mode fractures in viable reservoir rocks using a combination of new measuring techniques. The main results are summarized as follows:

- The opening-mode (calcite-filled and unfilled) fractures of the Arab carbonate reservoirs exhibit moderate to high roughness between 5 and 15 on the JRC scale. The smooth and rough fractures have matching walls, and only a minority of the rough fractures exhibit an obvious wall mismatch.
- The roughness and mismatch of the fracture walls reflect the lithology of the host carbonates and therefore are considered “fabric-dependent,” to be distinguished from the roughness produced by rock sliding and friction. The values of roughness are higher in coarse-grained rock and lower in fine-grained rock and can accordingly be predicted from describing the carbonate lithofacies such as mudstones, packstones, grainstones, and rudstones.
- Wall mismatch measurements of unfilled fractures from core are correlated with the aperture measurements from the borehole images. The results indicate that most of the NW-SE fractures (that are normal to the S_{Hmax}) are mechanically closed. The pressurized drilling fluids could not enter into the fractures (no apertures), and hence the fractures were undetected in borehole images. Nevertheless, a minority of the NW-SE fractures were detected in borehole images and found to have mismatching walls from aperture measurements. This indicates that these fractures preserved some apertures under the tectonic compression in Eastern Arabia that closed the wall-matching fractures.

ACKNOWLEDGMENTS

We thank Saudi Aramco, especially the Reservoir Characterization Department, for funding this project, and for giving us the data and permission to publish this paper. This work is part of Fahmi's Ph.D. project at Oxford University. Support from Oxford's Department of Earth Sciences is highly appreciated. Many thanks go to previous reviewers, including Nick Barton, whose insightful comments improved this manuscript.

REFERENCES CITED

- Al-Fahmi, M.M., and Cartwright, J.A., 2015, Factors controlling wellbore imaging of fractures: San Francisco, California, American Geophysical Union, Fall Meeting 2015, abstract MR41C-2643.
- Al-Fahmi, M.M., Cooke, M.L., and Cole, J.C., 2014, Modeling of the Dammam outcrop fractures: Case study for fracture development in salt-cored structures: *GeoArabia: Journal of the Middle East Petroleum Geosciences*, v. 19, p. 49–80 <http://www.gulfpetrolink.com/geoarabia/index.php/ga/article/view/31988>.
- Al-Fahmi, M.M., Plesch, A., Shaw, J.H., and Cole, J.C., 2016, Restorations of faulted domes: *American Association of Petroleum Geologists Bulletin*, v. 100, p. 151–163, <https://doi.org/10.1306/08171514211>.
- Alghamdi, E.S., Mahmood, T., and Macpherson, K.A., 2016, Fractures and in-situ stresses in the Upper Jurassic Arab-D and Hanifa Formations, Khurais, Eastern Saudi Arabia: *American Association of Petroleum Geologists Search and Discovery article 90254* (©2016, Fractures: GEO-2016, 12th Middle East Geosciences Conference & Exhibition, Manama, Bahrain, 7–10 March 2016, p. 1).
- Ameen, M.S., 2014, Fracture and in-situ stress patterns and impact on performance in the Khuff structural prospects, eastern offshore Saudi Arabia: *Marine and Petroleum Geology*, v. 50, p. 166–184, <https://doi.org/10.1016/j.marpetgeo.2013.10.004>.
- Ameen, M.S., Smart, B.G.D., Somerville, J.M., Hammilton, S., and Naji, N.A., 2009, Predicting rock mechanical properties of carbonates from wireline logs (A case study: Arab-D reservoir, Ghawar field, Saudi Arabia): *Marine and Petroleum Geology*, v. 26, p. 430–444, <https://doi.org/10.1016/j.marpetgeo.2009.01.017>.
- Ameen, M.S., Buhidma, I.M., and Rahim, Z., 2010, The function of fractures and in-situ stresses in the Khuff reservoir performance, onshore fields, Saudi Arabia: *American Association of Petroleum Geologists Bulletin*, v. 94, p. 27–60, <https://doi.org/10.1306/06160909012>.
- Barton, C.A., Zoback, M.D., and Moos, D., 1995, Fluid flow along potentially active faults in crystalline rock: *Geology*, v. 23, p. 683, [https://doi.org/10.1130/0091-7613\(1995\)023<0683:FFAPAF>2.3.CO;2](https://doi.org/10.1130/0091-7613(1995)023<0683:FFAPAF>2.3.CO;2).
- Barton, N., 2013, Shear strength criteria for rock, rock joints, rockfill and rock masses: Problems and some solutions: *Journal of Rock Mechanics and Geotechnical Engineering*, v. 5, p. 249–261, <https://doi.org/10.1016/j.jrmge.2013.05.008>.
- Barton, N., and Choubey, V., 1977, The shear strength of rock joints in theory and practice: *Rock Mechanics Felsmechanik Mecanique des Roches*, v. 10, p. 1–54, <https://doi.org/10.1007/BF01261801>.
- Barton, N., Bandis, S., and Bakhtar, K., 1985, Strength, deformation and conductivity coupling of rock joints: *International Journal of Rock Mechanics and Mining Sciences & Geomechanics Abstracts*, v. 22, p. 121–140, [https://doi.org/10.1016/0148-9062\(85\)93227-9](https://doi.org/10.1016/0148-9062(85)93227-9).
- Brown, S.R., 1987, Fluid flow through rock joints: The effect of surface roughness: *Journal of Geophysical Research*, v. 92, p. 1337–1347, <https://doi.org/10.1029/JB092iB02p01337>.
- Candela, T., Renard, F., Bouchon, M., Brouste, A., Marsan, D., Schmittbuhl, J., and Voisin, C., 2009, Characterization of fault roughness at various scales: Implications of three-dimensional high resolution topography measurements: *Pure and Applied Geophysics*, v. 166, p. 1817–1851, <https://doi.org/10.1007/s00024-009-0521-2>.
- Dunham, R.J., 1962, Classification of carbonate rocks according to depositional texture, in *M1: Classification of Carbonate Rocks—A Symposium*, p. 23.
- Haneberg, W., 2007, Directional roughness profiles from three-dimensional photogrammetric or laser scanner point clouds, in Eberhardt, E., Stead, D., Morrison, T., eds., *Rock Mechanics: Meeting Society's Challenges and Demands*: London, Taylor & Francis, p. 101–106, <https://doi.org/10.1201/NOE0415444019-c13>.
- Lee, Y.-H., Carr, J.R., Barr, D.J., and Haas, C.J., 1990, The fractal dimension as a measure of the roughness of rock discontinuity profiles: *International Journal of Rock Mechanics and Mining Sciences & Geomechanics Abstracts*, v. 27, p. 453–464, [https://doi.org/10.1016/0148-9062\(90\)90998-H](https://doi.org/10.1016/0148-9062(90)90998-H).
- Li, Y., and Zhang, Y., 2015, Quantitative estimation of joint roughness coefficient using statistical parameters: *International Journal of Rock Mechanics and Mining Sciences*, v. 77, p. 27–35, <https://doi.org/10.1016/j.ijrmms.2015.03.016>.
- Luthi, S.M., and Souhaité, P., 1990, Fracture apertures from electrical borehole scans: *Geophysics*, v. 55, p. 821–833, <https://doi.org/10.1190/1.1442896>.
- Luthy, S.T., and Grover, G.A., 1995, Three dimensional geologic modelling of a fractured reservoir, Saudi Arabia, in *Proceedings of Middle East Oil Show: Manama, Bahran*, p. 419–430, <https://doi.org/10.2118/29814-MS>.
- MacPherson, K.A.T., and Ameen, M.S., 2014, Fractures in the Jurassic Arab formation and Lower Fadhili carbonate member of the Dhurma Formation, Saudi Arabia, in *76th European Association of Geoscientists and Engineers (EAGE) Conference & Exhibition 2014 (16–19 June 2014)*: Amsterdam, Netherlands, p. 16–19.
- Maerz, N.H., Franklin, J.A., and Bennett, C.P., 1990, Joint roughness measurement using shadow profilometry: *International Journal of Rock Mechanics and Mining Sciences & Geomechanics Abstracts*, v. 27, p. 329–343, [https://doi.org/10.1016/0148-9062\(90\)92708-M](https://doi.org/10.1016/0148-9062(90)92708-M).
- Mitchell, J.C., Lehmann, P.J., Cantrell, D.L., Al-Jallal, I.A., and Al-Tagafy, M.A.R., 1988, Lithofacies, diagenesis and depositional sequence: Arab-D Member, Ghawar Field, Saudi Arabia, in Lomando, A.J., and Harris, P.M., eds., *Giant Oil and Gas Fields—A Core Workshop: Society of Economic Paleontologists and Mineralogists Core Workshop 12*, p. 459–514.
- Myers, N.O., 1962, Characterization of surface roughness: *Wear*, v. 5, p. 182–189, [https://doi.org/10.1016/0043-1648\(62\)90002-9](https://doi.org/10.1016/0043-1648(62)90002-9).
- Olsson, R., and Barton, N., 2001, An improved model for hydromechanical coupling during shearing of rock joints: *International Journal of Rock Mechanics and Mining Sciences*, v. 38, p. 317–329, [https://doi.org/10.1016/S1365-1609\(00\)00079-4](https://doi.org/10.1016/S1365-1609(00)00079-4).
- Sagy, A., Brodsky, E.E., and Axen, G.J., 2007, Evolution of fault-surface roughness with slip: *Geology*, v. 35, p. 283–286, <https://doi.org/10.1130/G23235A.1>.
- Schmittbuhl, J., Gentier, S., and Roux, S., 1993, Field measurements of the roughness of fault surfaces: *Geophysical Research Letters*, v. 20, p. 639–641, <https://doi.org/10.1029/93GL00170>.
- Tatone, B.S.A., and Grasselli, G., 2010, A new 2D discontinuity roughness parameter and its correlation with JRC: *International Journal of Rock Mechanics and Mining Sciences*, v. 47, p. 1391–1400, <https://doi.org/10.1016/j.ijrmms.2010.06.006>.
- Tagafy, M., Aramco, S., Subaie, A., Aramco, S., Ozkaya, S., and Contractor, S.A., 2017, Predictive fracture modeling: Example fields from Saudi Arabia, in *The Society of Petroleum Engineers–Kingdom of Saudi Arabia Section (SPE-KSA) Annual Technical Symposium and Exhibition, Saudi Arabia, 24–27 April 2017: Society of Petroleum Engineers*, p. 1–29.
- Weissbach, G., 1978, A new method for the determination of the roughness of rock joints in the laboratory: *International Journal of Rock Mechanics and Mining Sciences & Geomechanics Abstracts*, v. 15, p. 131–133, [https://doi.org/10.1016/0148-9062\(78\)90007-4](https://doi.org/10.1016/0148-9062(78)90007-4).
- Younessi, A., and Rasouli, V., 2010, A fracture sliding potential index for wellbore stability analysis: *International Journal of Rock Mechanics and Mining Sciences*, v. 47, p. 927–939, <https://doi.org/10.1016/j.ijrmms.2010.05.014>.
- Zhao, J., 1997, Joint surface matching and shear strength part A: Joint matching coefficient (JMC): *International Journal of Rock Mechanics and Mining Sciences*, v. 34, p. 173–178, [https://doi.org/10.1016/S0148-9062\(96\)00062-9](https://doi.org/10.1016/S0148-9062(96)00062-9).
- Zoback, M.D., 2007, *Reservoir Geomechanics*: Cambridge, UK, Cambridge University Press, 505 p., <https://doi.org/10.1017/CBO9780511586477>.